HHS Public Access

Author manuscript

Clin Cancer Res. Author manuscript; available in PMC 2018 January 01.

Published in final edited form as:

Clin Cancer Res. 2017 January 01; 23(1): 204–213. doi:10.1158/1078-0432.CCR-15-1601.

Identification of existing drugs that effectively target *NTRK1*- and *ROS1*-rearrangements in lung cancer

Curtis R. Chong[a], **Magda Bahcall**[a], **Marzia Capelletti**[a], **Takayuki Kosaka**[a], **Dalia Ercan**[a], **Taebo Sim**[b,c], **Lynette M. Sholl**[d], **Mizuki Nishino**[e], **Bruce E. Johnson**[a], **Nathanael S. Gray**[f,*], and **Pasi A. Jänne**[a,g,*]

[a]Lowe Center for Thoracic Oncology, Dana-Farber Cancer Institute, Boston, MA 02215

[b]Chemical Kinomics Research Center, Korea Institute of Science and Technology, Seoul, 136-791, Republic of Korea

[c]KU-KIST Graduate School of Converging Science and Technology, Seoul, 136-713, Republic of Korea

[d]Department of Pathology, Brigham and Women's Hospital, Boston, MA 02115

[e]Department of Radiology, Brigham and Women's Hospital, Boston, MA 02115, and Dana- Farber Cancer Institute, Boston, MA 02215

[f]Department of Biological Chemistry and Molecular Pharmacology, Harvard Medical School, and Department of Cancer Biology, Dana-Farber Cancer Institute, Boston MA, 02215

[g]Belfer Center for Applied Cancer Science, Dana-Farber Cancer Institute, Boston, MA 02215

Abstract

Purpose—Efforts to discover drugs that overcome resistance to targeted therapies in patients with rare oncogenic alterations, such as *NTRK1*- and *ROS1*-rearrangements, are complicated by the cost and protracted timeline of drug discovery.

Experimental design—In an effort to identify inhibitors of NTRK1 and ROS1, which are aberrantly activated in some patients with non-small cell lung cancer (NSCLC), we created and screened a library of existing targeted drugs against Ba/F3 cells transformed with these oncogenes.

Results—This screen identified the FDA-approved drug cabozantinib as a potent inhibitor of *CD74-ROS1* transformed Ba/F3, including the crizotinib-resistant mutants G2032R and L2026M (IC_{50} = 9, 26, and 11 nM, respectively). Cabozantinib inhibited *CD74-ROS1*-transformed Ba/F3 cells more potently than brigatinib (wild-type/G2032R/L2026M IC_{50} = 30/170/200 nM, respectively), entrectinib (IC_{50} = 6/2,200/3,500 nM), and PF-06463922 (IC_{50} = 1/270/2 nM). Cabozantinib inhibited ROS1 autophosphorylation and downstream ERK activation in transformed Ba/F3 cells and in patient-derived tumor cell lines. The IGF-1R inhibitor BMS-536924, potently inhibited *CD74-NTRK1* transformed compared to parental Ba/F3 cells (IC_{50} = 19 nM vs. > 470

*Address correspondence to either: Pasi A. Jänne, MD, PhD, Lowe Center for Thoracic Oncology, Dana-Farber Cancer Institute, 450 Brookline Avenue, LC4114, Boston, MA 02215, Phone: (617) 632-6076, Fax: (617) 582-7683, pasi_janne@dfci.harvard.edu. Nathanael S. Gray, PhD, Department of Biological Chemistry and Molecular Pharmacology, 360 Longwood Avenue, Longwood Center, Room 2209, Boston, MA 02215, Phone: (617) 582-8590, Fax: (617) 582-8615, Nathanael_Gray@dfci.harvard.edu.

nM). A patient with metastatic *ROS1*-rearranged NSCLC with progression on crizotinib was treated with cabozantinib and experienced a partial response.

Conclusions—While acquired resistance to targeted therapies is challenging, this study highlights that existing agents may be repurposed to overcome drug resistance, and identifies cabozantinib as a promising treatment of ROS1-rearranged NSCLC after progression on crizotinib.

Keywords

Lung cancer; drug screening

INTRODUCTION

Oncogenic driver mutations are found in approximately 50% of patients with non-small cell lung cancer (NSCLC) (1). Patients with activating mutations in *EGFR* or *ALK*-rearrangements respond to targeted therapies like erlotinib and crizotinib, respectively, but the development of resistance ultimately limits the clinical efficacy of these drugs (2). Beyond the more common NSCLC driver mutations in *EGFR* and *KRAS*, and *ALK*-rearrangements, a significant, but albeit smaller, group of patients are found to have alterations in *ROS1*, *NTRK1*, *HER2*, *BRAF*, *RET*, and *MET* (1).

The identification and regulatory approval of new therapies directed against less common oncogenic drivers, and any resistance mechanisms that may emerge, is complicated by the high cost and protracted time required to develop a new drug. Development of a new cancer drug, including highly targeted agents, may take up to 7 years and cost tens of millions of dollars (3). This presents a challenge to the treatment of patients with rare oncogenic drivers in lung cancer, who will eventually succumb to disease progression due to different mechanisms of acquired resistance.

One way to address this problem is to identify new uses for existing drugs. Because the clinical and pharmacologic properties of existing drugs are defined, any new use may rapidly be brought to the clinic. Examples of off-target inhibition by kinase inhibitors include crizotinib, which was initially developed to target MET, and later found to block ALK and ROS1 (4, 5), and imatinib, initially developed against ABL, and later found to inhibit PDGFR and KIT (6).

ROS1 was first reported as a potential driver oncogene in NSCLC in 2012. Patients with *ROS1*-rearrangements comprise approximately 1–3% of all NSCLC (5). Chromosomal rearrangement with a variety of partners leads to constitutive activation of ROS1, and the hybrid kinase is able to drive proliferation of oncogene-dependent cells (5). In addition to NSCLCs, *ROS1*-rearrangements are reported in glioblastoma, cholangiocarcinoma, gastric adenocarcinoma, ovarian serous tumors, inflammatory myofibroblastic tumors, and chronic myelomonocytic leukemia (7).

After preclinical studies demonstrated crizotinib inhibits ROS1 kinase (5, 8), a phase II study of NSCLC patients with *ROS1*-rearrangements treated with crizotinib was initiated. This study demonstrated an impressive 72% response rate to crizotinib treatment with a 19.2

month progression-free survival (9). Despite the success of crizotinib in *ROS1*-rearranged NSCLC, patients inevitably develop acquired resistance either through the L2026M "gatekeeper" mutation, alteration of another active site residue (G2032R), or undefined changes (10).

A number of methods have been used to design more potent inhibitors or to overcome crizotinib resistance in *ROS1*-rearranged NSCLC, including *de novo* drug discovery (11) and screens of existing kinase inhibitors (12, 13). The c-MET and VEGFR-2 inhibitor foretinib potently inhibits wild-type and G2032R-mutant *ROS1* (12). Foretinib reached phase II clinical trials in breast and lung cancer. However, because of its lack of clinical activity in unselected populations, its clinical development was discontinued. There are two ROS1 specific inhibitors undergoing clinical development: the dual ALK1/ROS1 inhibitor PF-06463922 (NCT01970865) and entrectinib (RXDX-101/NMS E628), a pan-TRK, ALK, and ROS1 inhibitor (STARTRK-1, NCT02097810).

NTRK1 (TRKA, neurotrophic tyrosine kinase receptor 1) fusions with different partners, including *CD74* and *MPRIP*, were identified in lung cancer in 2013. *NTRK1* rearrangements are thought to occur in 1–3% of patients with NSCLC (14). Under normal circumstances, the TRK family of kinases play a role in the development of the central and peripheral nervous systems and in pain sensation (15). *NTRK1* fusions have also been identified in thyroid, colon and ovarian cancer, melanoma, cholangiocarcinoma, glioblastoma, and acute myeloid leukemia (15). The activity of the fusion kinase is inhibited by crizotinib and lestaurtinib, and TRK-specific inhibitors such as entrectinib, AZD7451, and ARRY-470 are among at least 9 compounds undergoing clinical development.

In an effort to further accelerate development of drugs that target ROS1 and NTRK1 in lung cancer, including resistant variants of ROS1, a library of existing targeted therapies was screened for inhibition of these two kinases. The collection of existing targeted therapies includes 290 compounds that target 104 different signaling pathways (Supplementary Figure 1, Supplementary File 1), and are in different stages of clinical development, from preclinical to FDA-approved. To discover ROS1 and NTRK1 kinase inhibitors this collection, the Dana-Farber Targeted Therapy Library, was used to assess the antiproliferative activity on the oncogene-dependent cell line Ba/F3 transformed with either *CD74-ROS1* or *CD74-NTRK1*. We selected a repurposing strategy because, in contrast to *ALK*-rearranged and *EGFR*-mutant NSCLCs, for which 2nd and 3rd generation inhibitors that overcome resistance have entered the clinic (16, 17), no such targeted 2nd-line therapies exist for patients with *ROS1*-rearrangements after progression on crizotinib.

MATERIALS AND METHODS

Proliferation assays

Ba/F3 cells (immortalized murine bone-marrow derived pro-B cells) transfected with either *CD74-ROS1* or *CD74-NTRK1* were used for screening and were prepared as previously described (14). An expanded version of the KIN001 library, which is composed of commercially-available and in-house kinase inhibitors, was used for screening (18). High-throughput screening was performed in duplicate in 384-well plates with 1,000 cells/well

and a final DMSO concentration < 0.5%. Cells and drug were incubated for 72 hours, and viability was measured using CellTiter Glo. IC_{50} experiments were performed in triplicate, were calculated using a sigmoidal, non-linear dose-response model in GraphPad Prism, and are presented as the mean of 3 separate experiments. The CUTO-3 cell line was the generous gift of Dr. Robert C. Doebele. The UMG-118 and HCC-78 cell lines were obtained from the American Type Culture Collection (ATCC, Manassas, Virginia) and passaged in our laboratory for less than 6 months; ATCC uses short tandem repeat profiling for cell line authentication.

Western blot analysis

Cells were incubated with inhibitor for 6 hours. Cell lysate (prepared by 30 minute incubation with 0.1% Triton X-100 + protease inhibitor) was loaded into each well of a 4–12% Bis-Tris gel. Gels were transferred to PVDF membranes, blocked with 5% milk, and incubated with a 1:1,000 dilution of primary antibody and a 1:5,000 secondary antibody solution.

Structural modeling

Molecular docking studies of cabozantinib on the wild-type ROS1 and point-mutated (L2026M and G2032R) kinase domain were performed. In order to construct a homology model, structures of the wild-type ROS1 and point-mutated (L2026M and G2032R) ROS1 kinase domain, the 3D structure of the template kinase c-Met in the DFG out conformations (PDB accession code: 3LQ8) was retrieved from the Protein Data Bank. Sequence alignments of ROS1 and the template protein were generated using the Discovery Studio 4.1 package. 3D model structures of wild-type and point-mutated (L2026M and G2032R) ROS1 kinase domain were built-up using the Modeler in Discovery Studio 4.1 package, and were further refined by using the CHARMM force field. The 3D structure of cabozantinib was built using Maestro build panel and energy-minimized using the Impact module of Maestro in the Schrödinger suite program. Ligand docking onto the active site of wild-type and point-mutated (L2026M and G2032R) ROS1 kinase domain was carried out using the Schrödinger docking program, Glide. The best-docked poses were selected as the lowest Glide score.

Genetic profiling

OncoPANEL is a hybrid capture targeted next generation sequencing assay to detect somatic mutations, copy number variations and structural variants in tumor DNA extracted from fresh, frozen, or formalin-fixed paraffin-embedded samples (19). DNA was isolated from tissue containing at least 20% tumor nuclei and analyzed by massively parallel sequencing using a solution-phase Agilent SureSelect hybrid capture kit and an Illumina HiSeq 2500 sequencer. The studies were performed in a CLIA certified laboratory, and the resulting sequences were interpreted by a board-certified anatomic pathologist. The patient provided consent to clinical and research use of the genomic findings, which were approved by the Dana-Farber Harvard Cancer Center Institutional Review Board.

Creation of *NTRK1* gatekeeper mutation

The pDNR-dual plasmid containing wild-type *CD74-NTRK1* kinase was used for site directed mutagenesis of Phe589 to Val. The mutated *CD74-NTRK1* fusion was then transferred to the JP1540 vector using Cre recombination (New England Biolabs) and transformed into *E coli*. Plasmid was purified and then transfected using the FuGene reagent (Promega, Madison, Wisconsin) into 293 cells. Protein expression and kinase activity was assessed as described above.

RESULTS

Identification of targeted agents that inhibit ROS1 and NRTK1 kinase activity

A library of 290 agents that target 104 different cellular pathways was created (Supplementary Figure 1A and B, Supplementary File 1A). Compounds active against more than one pathway are represented for each unique target; for example, crizotinib is included as both a MET and ALK inhibitor. This collection, the Dana-Farber Targeted Therapy Library (DFTTL), contains 148 preclinical compounds (51%), 31 drugs that entered phase I clinical trials (11%), 50 drugs in phase II clinical trials (18%), 30 drugs tested in phase III clinical trials (10%), and 31 drugs approved by the U.S. Food and Drug Administration (FDA) (10%), including 25 of the 32 targeted agents approved by the FDA in cancer (78%). Others have screened libraries of targeted agents on ROS1 (12, 20), and the overlap between libraries is summarized in Supplementary Figure 2.

The DFTTL was screened at 1 μM concentration on Ba/F3 cells transformed with *CD74-ROS1* or *CD74-NTRK1* fusions; the parental Ba/F3 cell line grown in the presence of IL-3 was screened in parallel. A cut-off of 50% inhibition, represented as the %viability parental Ba/F3 - %viability transformed Ba/F3, was used to identify hits for further characterization. Ba/F3 cells have been extensively used in kinase drug discovery, including screens for compounds targeting kinases activated by rearrangement, such as ROS1 (12, 20, 21). Compounds showing > 50% inhibition for ROS1 (n = 44) and NTRK1 (n = 19) are shown by stage of clinical development in Figure 1, with IC_{50} values for hits available in Supplementary File 1B and 1C. Screen results by pathway are presented Supplementary Figure 3.

Identification of NTRK1 inhibitors

Dovitinib and BMS-536924 selectively inhibited the proliferation of *CD74-NTRK1* transformed Ba/F3 cells but not the parental, interleukin-dependent Ba/F3 cells (Figure 2A). Lestaurtinib (CEP-701) is a FLT3, JAK2, TrkA/B/C inhibitor structurally similar to staurosporine that is undergoing clinical trials in AML (22), and was used as a positive control for NTRK1 inhibition. Dovitinib is an FGFR3 inhibitor in phase III clinical trials for renal cell carcinoma that reaches a peak plasma level with oral dosing of 568 nM observed in clinical trials (23), and BMS-536924 is an ATP-competitive IGF1-1R inhibitor.

NTRK1 undergoes autophosphorylation at tyrosine residues 490, 674, and 675, and this leads to activation of ERK via phosphorylation (15). In NIH-3T3 cells transformed with FLAG-tagged *CD74-NTRK1,* both BMS-536924 and lestaurtinib inhibit NTRK1

autophosphorylation (Figure 2B). Inhibition of NTRK1 autophosphorylation by dovitinib was weaker than would be suggested by its IC_{50} value. The CUTO-3 cell line was derived from a patient with lung adenocarcinoma and contains an *MPRIP-NTRK1* rearrangement (14). BMS-536924, dovitinib, and lestaurtinib inhibited proliferation of CUTO-3 cells (IC_{50} = 34 nM, 170 nM, and 3 nM, respectively) (Figure 2C). As seen in 3T3 cells transformed with *CD74-NTRK1*, BMS-536924 and lestaurtinib inhibited NTRK1 autophosphorylation in CUTO-3 cells (Figure 2D). Dovitinib again showed partial inhibition of NTRK1 autophosphorylation at 1000 nM in CUTO-3 cells, suggesting that blockade of other targets may account for the inhibition observed.

Mutations in the active site “gatekeeper” residue decrease or abolish the efficacy of inhibitors that bind to the active site of may kinases. The residue Phe589 was identified as the putative gatekeeper residue in the NTRK1 kinase active site based on the available crystal structure (Figure 2E). This residue was mutated to valine, and the effect of inhibitors identified in our screen were assessed on NTRK1 autophosphorylation in 293 cells transiently transfected with both wild-type and F589V *CD74-NTRK1*. As seen in Figure 2F, the F589V mutation did not affect inhibition of NTRK1 autophosphorylation by lestaurtinib or BMS-536924.

Lead compounds inhibit ROS1 signaling

The most potent agents identified were cabozantinib, foretinib, and brigatinib (AP26113) for ROS1, with little inhibition seen of the parental Ba/F3 cells by these compounds (Figure 3, Table 1, Supplementary Figure 4). Cabozantinib and foretinib exhibited potent activity against both wild-type ROS1 and the two reported kinase mutants that confer acquired resistance to crizotinib, the G2032R and L2026M mutations, as previously reported (20). In contrast, PF-06463922, which is in phase II clinical trials of *ALK*- and *ROS1*-rearranged NSCLC, potently inhibited wild-type and L2026M mutant ROS1, but demonstrated > 250-fold less potent inhibition of the G2032R mutant. Entrectinib inhibited wild-type ROS1 with an IC_{50} of 6 nM, with little inhibition (IC_{50} > 1 μM) seen for the G2032R or L2026M mutants.

ROS1 undergoes autophosphorylation at tyrosine 2274, and this stimulates cell proliferation via activation of multiple downstream pathways including ERK, PI3K, and AKT (7). When *CD74-ROS1* wild-type, G2032R or L2026M transformed Ba/F3 cells are incubated with increasing concentrations of cabozantinib or foretinib, a decrease is seen in the phosphorylation of ROS1 and ERK (Figure 3B). In contrast, crizotinib inhibits the phosphorylation of ROS1 and ERK in the wild-type *CD74-ROS1* Ba/F3 cells only. Brigatinib inhibits the phosphorylation of ROS1 and ERK in *CD74-ROS1* wild-type and L2026M mutant transformed Ba/F3 cells, with less activity seen in the *CD74-ROS1* G2032R transformed Ba/F3 cells. PF-06463922 inhibited wild-type and L2026M mutant ROS1 autophosphorylation and ERK activation, with little effect on signaling in the G2032R mutant, and entrectinib was only effective at blocking activity of wild-type ROS1 signaling (Supplementary Figure 5).

Inhibition of ROS1 signaling in human cancer cells bearing *ROS1*-rearrangements

The effect of cabozantinib, crizotinib, and foretinib were next studied in the NSCLC HCC78 cell line, which expresses the *SLC34A2-ROS1* fusion, and in the UMG-118 glioblastoma cell line, which expresses the *FIG-ROS1* fusion. As seen in the *CD74-ROS1* transformed Ba/F3 cells, brigatinib, cabozantinib, crizotinib, and foretinib showed similar inhibition of HCC78 proliferation (Figure 3C), ROS1 autophosphorylation, and downstream ERK activation (Figure 3D). The IC_{50} for inhibition of HCC78 observed for these drugs is similar to that reported by others (12), and is up to ~150-fold less potent than in *CD74-ROS1*-transformed Ba/F3 cells, likely due to activation of other signaling pathways. Inhibition of ROS1 autophosphorylation and ERK activation is also seen in the UMG-118 cell line (Supplementary Figure 6).

Modeling of cabozantinib in the ROS1 active site reveals the molecular basis for inhibition of wild-type and mutant kinase

To define the molecular basis for the inhibition, cabozantinib was modeled into the active site of ROS1 (Figure 3E). In this structure, the quinoline nitrogen of cabozantinib makes a hinge contact with Met2029, an amide group attached to the bridge phenyl ring forms a pair of hydrogen bonds with the backbone carbonyl group of Gly2101 and the ε-amino group of Lys1980. Further contacts are made with a hydrogen bond between the amide group attached to the tail phenyl ring and the carboxyl group of Asp2102, and a π-π stacking interaction between the phenyl ring and Phe2103. In G2032R and L2026M mutant ROS1, while there is no hydrogen bond between the amide group attached to the tail phenyl ring and the carboxyl group of Asp2102, the other interactions are preserved. By preserving most of the interactions seen in the wild-type kinase, cabozantinib is able to achieve potent inhibition of both the G2032R and L2026M mutants.

Cabozantinib demonstrates antitumor activity in a patient with *ROS1*-rearranged NSCLC who progressed on crizotinib and multiple lines of cytotoxic chemotherapy

Given the efficacy of cabozantinib in preclinical models of *ROS1*-rearranged NSCLC, a 53 year-old woman with *ROS1*-rearranged metastatic lung adenocarcinoma who developed acquired resistance to crizotinib was identified and eventually treated with cabozantinib. The patient was a never smoker who presented with cough and fatigue in November 2011, and was found to have diffuse tumor involvement of the left lung with extensive mediastinal adenopathy, enlarged intra-abdominal lymph nodes, and a single metastasis in the liver (T4N3M1b). She underwent 6 cycles of cisplatin + pemetrexed followed by 6 cycles of maintenance pemetrexed with a partial response. After progression in October 2012 she received 6 cycles of carboplatin + gemcitabine with erlotinib maintenance. Crizotinib treatment was initiated in September 2013 after biopsy of a left lower lobe nodule done following progression on erlotinib revealed a *ROS1*-rearrangement in 18 of 50 nuclei. Restaging scans showed a partial response, which lasted until October 2014 when she developed worsening dyspnea and cough. A computed tomography scan showed multiple new pulmonary nodules and opacities as well as a dominant mass in the left upper lobe (Figure 4A, B), and thoracentesis yielded 2.5 L of malignant pleural fluid.

In December 2014 she was initiated on cabozantinib at 140 mg daily, based on the preclinical work by us and others (20) demonstrating inhibition of the wild-type, G2032R, and L2026M ROS1 kinase. The patient was informed of the off-label use of cabozantinib. Approximately two weeks later, the dose was reduced to 120 mg daily, then 80 mg daily, and then cabozantinib was held after approximately 3 weeks on treatment due to grade III palmar-plantar erythrodysesthesia and grade II fatigue. A CT scan performed because of dyspnea 4 weeks after initiation of cabozantinib revealed bilateral segmental pulmonary emboli and resolution of the dominant mass in the left upper lobe, which had previously measured 4.3 cm, and reduction in the right lower lobe lesion from 1.7 cm to 1.4 cm (Figure 4C, D). The pulmonary embolism was medically managed, and the palmar-plantar erythrodysesthesia improved with the use of gabapentin, urea cream, and clobetasol. Cabozantinib was restarted at 20 mg daily. A repeat chest CT scan performed two weeks later and approximately 8 weeks after initiation of cabozantinib treatment demonstrated maintenance of the disease response with slightly increased bilateral pleural effusions. The cabozantinib dose was subsequently increased to 40 mg daily. After uptitration of the dose to 60 mg daily, the grade III palmar-plantar erythrodysesthesia returned, and the patient elected to discontinue cabozantinib. She subsequently showed symptomatic and radiographic disease progression, approximately 10 weeks after initiating cabozantinib, and 3 weeks after its discontinuation.

Sequencing of tumor cells from the effusion that developed after crizotinib resistance revealed a wild-type *ROS1* kinase domain, rearrangement of *ROS1* intron 33 with *RNPC3* intron 12 (Supplementary Figure 7) and *EZR* intron 10, and other genomic alterations of unclear significance. In this patient, the *ROS1* translocation may involve a *ROS1* (exon1-33)-RNPC (exon 12–15) fusion and an *EZR-ROS1* (exon 34-43) fusion. The *EZR-ROS1* fusion is commonly observed in patients with *ROS1*-rearranged NSCLC and is predicted to be oncogenic as the ROS1 kinase domain is located after exon 36 (7).

DISCUSSION

To accelerate discovery of new therapeutics for *ROS1*- and *NTRK1*-rearranged lung cancer, a library of existing targeted agents was screened. Compounds were selected for further study based on potency, selectivity, and clinical availability.

Cabozantinib was the most promising ROS1 inhibitor identified because it inhibits both the wild-type ROS1 and the G2032R and L2026M mutants that confer resistance to crizotinib. Unlike brigatinib, entrectinib, and PF-06463922, three drugs in clinical development as ROS1 inhibitors, cabozantinib is equally potent against wild-type and crizotinib-resistant (G2032R and L2026M) ROS1. Brigatinib and PF-06463922 were not present in our initial library, and were used to compare the efficacy of inhibition of wild-type ROS1 and the G2032R and L2026M mutations with cabozantinib. Cabozantinib is able to achieve potent inhibition of wild-type and crizotinib-resistant ROS1 by maintaining most of the interactions in the enzyme active site.

Cabozantinib is currently FDA-approved for the treatment of medullary thyroid carcinoma. Kinase inhibition occurs at concentrations ~50-fold less than the peak plasma level obtained

through FDA-approved oral dosing (Table 1). As an FDA-approved drug, cabozantinib has been extensively studied in the clinic. In medullary thyroid cancer, cabozantinib increases the progression-free survival (11.2 months vs. 4 months) compared to placebo (24). Cabozantinib has also been studied in prostate cancer (25), *RET*-rearranged NSCLC, and renal cell carcinoma (26). Of 3 patients with *RET*-rearranged NSCLC treated with cabozantinib, 2 experienced a partial response and 1 patient had stable disease (27). In the phase III thyroid cancer study, adverse events including diarrhea, palmar-plantar erythrodysesthesia, weight loss, anorexia, and fatigue led to dose-reductions or discontinuation in 79% and 16% of patients, respectively (24).

Based on the preclinical work presented here and in the available literature (20), off-label cabozantinib treatment was used in a *ROS1*-rearranged NSCLC patient who had progressed after 13 months of crizotinib treatment and 3 other forms of systemic therapy. Cabozantinib was chosen over cytotoxic chemotherapy because the patient's lung cancer had previously progressed on cisplatin + pemetrexed, carboplatin + gemcitabine, erlotinib, and crizotinib. The FDA-approved dose of 140 mg daily was chosen given the patient's symptomatic progression on crizotinib. Her symptoms of cough and dyspnea rapidly improved on the 140 mg cabozantinib dose, and radiographic improvement was apparent 4 weeks later. This is consistent with the prompt responses seen to erlotinib/gefitinib and crizotinib in *EGFR* mutant and *ALK*-rearranged NSCLC.

Unfortunately, it appeared that the therapeutic window of cabozantinib overlapped with toxic levels in our patient. In the clinical trial of cabozantinib in medullary thyroid cancer, 79% of patients had dose reductions, and 65% of patients had doses held (24). The clinical trial of cabozantinib in prostate cancer attempted to address this issue by using either 40 mg or 100 mg doses (25). The rate of dose reduction was 84% in the 100 mg group and 31% in the 40 mg group, with discontinuation rates of 25% and 18%, respectively.

Ceritinib, an ALK inhibitor, is effective in crizotinib resistant cancers that do or do not contain an ALK secondary mutation (17). The activity in the latter subgroup may be due to either the increased potency of ceritinib on ALK and/or the inhibition of other kinases such as IGFR1 inhibited by ceritinib but not crizotinib (28). Analogously, the increased potency of cabozantinib on ROS1 may be the reason for the clinical benefit in our patient.

Analysis of the patient's tumor DNA using targeted next generation sequencing did not reveal any variants that could explain resistance to crizotinib. Specifically, we did not identify in our patient the G2032R or L2026M mutations that confer resistance to crizotinib, while maintaining sensitivity to cabozantinib. In patients with *EGFR*-mutant NSCLC and progression on an EGFR TKI, cabozantinib 40 mg daily with erlotinib resulted in an 11% response rate (29), and this was attributed to targeting of resistance pathways including MET. It is possible that cabozantinib was active against a secondary pathway that caused resistance, in addition to more potently inhibiting wild-type ROS1 kinase.

Our patient had two *ROS1*-rearrangements involving intron 33 with *EZR*, which has previously been reported (9), and with *RNPC3* (RNA-binding region containing 3) on chromosome 1p21, which, to our knowledge, has not been previously reported. *CD74* is the

most common *ROS1* fusion partner among the 11 different partners that have been reported (7, 9). The *RNPC3* gene encodes a 517 amino acid protein, RNA binding protein 40 (also known as U11/U12 snRNP 65k), that is a component of the U12-dependent (minor) spliceosome (30). This protein complex removes U12-type introns, which are thought to comprise < 0.1% of all human introns (30). The relative abundance of tumor cells with the *EZR-ROS1* and *RNPC3-ROS1* fusion is unclear, as is whether both are expressed in tumor cells versus a heterogeneous population of tumor cells expressing either the *EZR* or *RNPC* fusion.

Based on our preclinical and clinical observations, a potential future clinical trial should be initiated to specifically to examine the efficacy of cabozantinib in patients with progression on crizotinib. If *ROS1*-rearrangements comprise 1–3% of all NSCLC, this population could include nearly 7,000 patients annually in the U.S, and a substantially larger number around the world.

Our screen also identified BMS-536924 as a potential NTRK1 inhibitor. Mutation of the putative gatekeeper Phe589 (F589V) failed to abrogate inhibition of NTRK1 autophosphorylation for both BMS-536924 and lestaurtinib in 293 cells transformed with mutant *CD74-NTRK1*, suggesting that both agents may still retain the ability to inhibit NTRK1 and downstream signaling including ERK even in the presence of the gatekeeper mutation. A second potential explanation for these observations is that inhibition of *CD74-NTRK1* F589V Ba/F3 cells by BMS-536924 and lestaurtinib is due to an off-target effect of these inhibitors. In order to differentiate between these two possibilities additional biochemical studies, to determine binding of BMS-536924 and lestaurtinib to NTRK1 and NTRK1 F589V, and mutagenesis studies, to introduce additional gatekeeper residues and solvent front mutations, will need to be performed. Given the ATP binding site homology observed amongst NTRK family members (31), the inhibitors reported here could be tested for inhibition of NTRK2 and NTRK3 in future studies.

Genetic sequencing efforts are identifying ever more rare subsets of patients with actionable driver oncogenes. The identification of new uses for existing targeted therapies in such patients is a way to rapidly deliver new treatments to the clinic, while avoiding the high cost of *de novo* drug development. This strategy may also be deployed to overcome resistance to targeted therapies across a variety of oncogene-addicted cancers. As new uses are discovered for existing targeted therapies, patients should be encouraged to participate in clinical trials of these agents, rather than be used as a rationale for off-protocol, non-trial use of such drugs.

Supplementary Material

Refer to Web version on PubMed Central for supplementary material.

Acknowledgments

This study is supported by grants from the National Institutes of Health RO1CA136851 (P.A.J. and N.S.G.), R01CA135257 (P.A.J.), 1K23CA157631 (M.N.) and 1 U54 HL127365-01 (N.S.G.), the Cammarata Family Foundation Research Fund (M.C. and P.A.J.), and the Nirenberg Fellowship at Dana-Farber Cancer Institute (M.C. and P.A.J.). C.R.C is the recipient of funding from Uniting Against Lung Cancer, a Conquer Cancer Foundation/

ASCO Young Investigator Award, and a post-doctoral fellowship from the American Cancer Society (PF-14-020-01-CDD).

References

1. Kris MG, Johnson BE, Berry LD, Kwiatkowski DJ, Iafrate AJ, Wistuba II, et al. Using multiplexed assays of oncogenic drivers in lung cancers to select targeted drugs. Jama. 2014; 311:1998–2006. [PubMed: 24846037]
2. Chong CR, Janne PA. The quest to overcome resistance to EGFR-targeted therapies in cancer. Nat Med. 2013; 19:1389–400. [PubMed: 24202392]
3. Chabner BA. Early accelerated approval for highly targeted cancer drugs. N Engl J Med. 2011; 364:1087–9. [PubMed: 21428763]
4. Timofeevski SL, McTigue MA, Ryan K, Cui J, Zou HY, Zhu JX, et al. Enzymatic characterization of c-Met receptor tyrosine kinase oncogenic mutants and kinetic studies with aminopyridine and triazolopyrazine inhibitors. Biochemistry. 2009; 48:5339–49. [PubMed: 19459657]
5. Bergethon K, Shaw AT, Ou SH, Katayama R, Lovly CM, McDonald NT, et al. ROS1 rearrangements define a unique molecular class of lung cancers. J Clin Oncol. 2012; 30:863–70. [PubMed: 22215748]
6. Demetri GD, von Mehren M, Blanke CD, Van den Abbeele AD, Eisenberg B, Roberts PJ, et al. Efficacy and safety of imatinib mesylate in advanced gastrointestinal stromal tumors. N Engl J Med. 2002; 347:472–80. [PubMed: 12181401]
7. Gainor JF, Shaw AT. Novel targets in non-small cell lung cancer: ROS1 and RET fusions. Oncologist. 2013; 18:865–75. [PubMed: 23814043]
8. Yasuda H, de Figueiredo-Pontes LL, Kobayashi S, Costa DB. Preclinical rationale for use of the clinically available multitargeted tyrosine kinase inhibitor crizotinib in ROS1-translocated lung cancer. J Thorac Oncol. 2012; 7:1086–90. [PubMed: 22617245]
9. Shaw AT, Ou SH, Bang YJ, Camidge DR, Solomon BJ, Salgia R, et al. Crizotinib in ROS1-rearranged non-small-cell lung cancer. N Engl J Med. 2014; 371:1963–71. [PubMed: 25264305]
10. Awad MM, Katayama R, McTigue M, Liu W, Deng YL, Brooun A, et al. Acquired resistance to crizotinib from a mutation in CD74-ROS1. N Engl J Med. 2013; 368:2395–401. [PubMed: 23724914]
11. Narayanan R, Yepuru M, Coss CC, Wu Z, Bauler MN, Barrett CM, et al. Discovery and preclinical characterization of novel small molecule TRK and ROS1 tyrosine kinase inhibitors for the treatment of cancer and inflammation. PLoS One. 2013; 8:e83380. [PubMed: 24386191]
12. Davare MA, Saborowski A, Eide CA, Tognon C, Smith RL, Elferich J, et al. Foretinib is a potent inhibitor of oncogenic ROS1 fusion proteins. Proc Natl Acad Sci U S A. 2013; 110:19519–24. [PubMed: 24218589]
13. Katayama R, Khan TM, Benes C, Lifshits E, Ebi H, Rivera VM, et al. Therapeutic strategies to overcome crizotinib resistance in non-small cell lung cancers harboring the fusion oncogene EML4-ALK. Proc Natl Acad Sci U S A. 2011; 108:7535–40. [PubMed: 21502504]
14. Vaishnavi A, Capelletti M, Le AT, Kako S, Butaney M, Ercan D, et al. Oncogenic and drug-sensitive NTRK1 rearrangements in lung cancer. Nat Med. 2013; 19:1469–72. [PubMed: 24162815]
15. Vaishnavi A, Le AT, Doebele RC. TRKing down an old oncogene in a new era of targeted therapy. Cancer Discov. 2015; 5:25–34. [PubMed: 25527197]
16. Janne PA, Yang JC, Kim DW, Planchard D, Ohe Y, Ramalingam SS, et al. AZD9291 in EGFR inhibitor-resistant non-small-cell lung cancer. N Engl J Med. 2015; 372:1689–99. [PubMed: 25923549]
17. Shaw AT, Kim DW, Mehra R, Tan DS, Felip E, Chow LQ, et al. Ceritinib in ALK-rearranged non-small-cell lung cancer. N Engl J Med. 2014; 370:1189–97. [PubMed: 24670165]
18. Weisberg E, Liu Q, Zhang X, Nelson E, Sattler M, Liu F, et al. Selective Akt inhibitors synergize with tyrosine kinase inhibitors and effectively override stroma-associated cytoprotection of mutant FLT3-positive AML cells. PLoS One. 2013; 8:e56473. [PubMed: 23437141]

19. Wagle N, Berger MF, Davis MJ, Blumenstiel B, Defelice M, Pochanard P, et al. High-throughput detection of actionable genomic alterations in clinical tumor samples by targeted, massively parallel sequencing. Cancer Discov. 2012; 2:82–93. [PubMed: 22585170]
20. Katayama R, Kobayashi Y, Friboulet L, Lockerman EL, Koike S, Shaw AT, et al. Cabozantinib Overcomes Crizotinib Resistance in ROS1 Fusion-Positive Cancer. Clin Cancer Res. 2015; 21:166–74. [PubMed: 25351743]
21. Warmuth M, Kim S, Gu XJ, Xia G, Adrian F. Ba/F3 cells and their use in kinase drug discovery. Curr Opin Oncol. 2007; 19:55–60. [PubMed: 17133113]
22. Knapper S, Burnett AK, Littlewood T, Kell WJ, Agrawal S, Chopra R, et al. A phase 2 trial of the FLT3 inhibitor lestaurtinib (CEP701) as first-line treatment for older patients with acute myeloid leukemia not considered fit for intensive chemotherapy. Blood. 2006; 108:3262–70. [PubMed: 16857985]
23. Kim KB, Chesney J, Robinson D, Gardner H, Shi MM, Kirkwood JM. Phase I/II and pharmacodynamic study of dovitinib (TKI258), an inhibitor of fibroblast growth factor receptors and VEGF receptors, in patients with advanced melanoma. Clin Cancer Res. 2011; 17:7451–61. [PubMed: 21976540]
24. Elisei R, Schlumberger MJ, Muller SP, Schoffski P, Brose MS, Shah MH, et al. Cabozantinib in progressive medullary thyroid cancer. J Clin Oncol. 2013; 31:3639–46. [PubMed: 24002501]
25. Smith MR, Sweeney CJ, Corn PG, Rathkopf DE, Smith DC, Hussain M, et al. Cabozantinib in Chemotherapy-Pretreated Metastatic Castration-Resistant Prostate Cancer: Results of a Phase II Nonrandomized Expansion Study. J Clin Oncol. 2014; 32:3391–9. [PubMed: 25225437]
26. Choueiri TK, Pal SK, McDermott DF, Morrissey S, Ferguson KC, Holland J, et al. A phase I study of cabozantinib (XL184) in patients with renal cell cancer. Ann Oncol. 2014; 25:1603–8. [PubMed: 24827131]
27. Drilon A, Wang L, Hasanovic A, Suehara Y, Lipson D, Stephens P, et al. Response to Cabozantinib in patients with RET fusion-positive lung adenocarcinomas. Cancer Discov. 2013; 3:630–5. [PubMed: 23533264]
28. Lovly CM, McDonald NT, Chen H, Ortiz-Cuaran S, Heukamp LC, Yan Y, et al. Rationale for co-targeting IGF-1R and ALK in ALK fusion-positive lung cancer. Nat Med. 2014; 20:1027–34. [PubMed: 25173427]
29. Reckamp KL, Frankel PH, Mack PC, Gitlitz BJ, Ruel N. Phase II trial of XL184 (cabozantinib) plus erlotinib in patients (pts) with advanced EGFR mutant non-small cell lung cancer (NSCLC) with progressive disease (PD) on epidermal growth factor receptor (EGFR) tyrosine kinase inhibitor (TKI) therapy: A California Cancer Consortium phase II trial (NCI 9303. J Clin Oncol. 2014; 32(suppl) abstr 8014.
30. Will CL, Schneider C, Hossbach M, Urlaub H, Rauhut R, Elbashir S, et al. The human 18S U11/U12 snRNP contains a set of novel proteins not found in the U2-dependent spliceosome. Rna. 2004; 10:929–41. [PubMed: 15146077]
31. Bertrand T, Kothe M, Liu J, Dupuy A, Rak A, Berne PF, et al. The crystal structures of TrkA and TrkB suggest key regions for achieving selective inhibition. J Mol Biol. 2012; 423:439–53. [PubMed: 22902478]

FINANCIAL DISCLOSURES

Identification of existing drugs that target *NTRK1*- and *ROS1*-rearrangements in lung cancer

C.R. Chong:

Other

(Major $10,000 or more) WolterKluwer Publishing

M. Bahcall

None

M. Capelletti

None

T. Kosaka

None

D. Ercan

None

T. Sim

None

L.M. Sholl:

Consultant/Advisory Board

(Minor $10,000 or less) Genentech

M. Nishino

Consultant/Advisory Board (Minor $10,000 or less) Bristol Myers Squibb

Other:

Research Grant from Canon Inc (paid to the institution, co-investigator)

B.E. Johnson:

Consultant/Advisory Board

(Major $10,000 or more) KEW Group

(Minor $10,000 or less) Merck and Eli Lilly

Ownership (Minor $10,000 or less) KEW Group

N.S. Gray:

Major:

Syros Pharma –founder, SAB member, developing IP from Dana Farber

(Minor $10,000 or less) Inventor on Dana Farber Cancer Institute owned patent on WZ4002, Stock ownership in Gatekeeper Pharmaceuticals

P.A. Jänne:

Consultant/Advisory Board (Minor $10,000 or less) Astra Zeneca, Boehringer Ingelheim, Pfizer, Genentech, Clovis Oncology, Merrimack Pharmaceuticals, Chugai, Sanofi

Other (Major $10,000 or more) Lab Corp – post-marketing royalties from DFCI owned intellectual property on EGFR mutations licensed to Lab Corp

(Minor $10,000 or less) Inventor on Dana Farber Cancer Institute owned patent on WZ4002, Stock ownership in Gatekeeper Pharmaceuticals

STATEMENT OF TRANSLATIONAL RELEVANCE

We identified cabozantinib as a potent inhibitor of wild-type ROS1 kinase and the L2026M and G2032R mutants that confer acquired clinical resistance to crizotinib by screening a library of existing targeted therapies. A patient with *ROS1*-rearranged NSCLC who progressed on crizotinib was treated with cabozantinib and experienced a partial response. Cabozantinib is a more potent inhibitor of G2032R and L2026M mutant, crizotinib-resistant ROS1 compared to brigatinib, entrectinib, and PF-06463922, and should be evaluated in *ROS1* rearranged crizotinib resistant patients. The identification of new uses for existing targeted therapies in such patients is a way to rapidly deliver new treatments to the clinic, while avoiding the high cost of *de novo* drug development. This strategy may also be deployed to overcome resistance to targeted therapies across a variety of oncogene-addicted cancers.

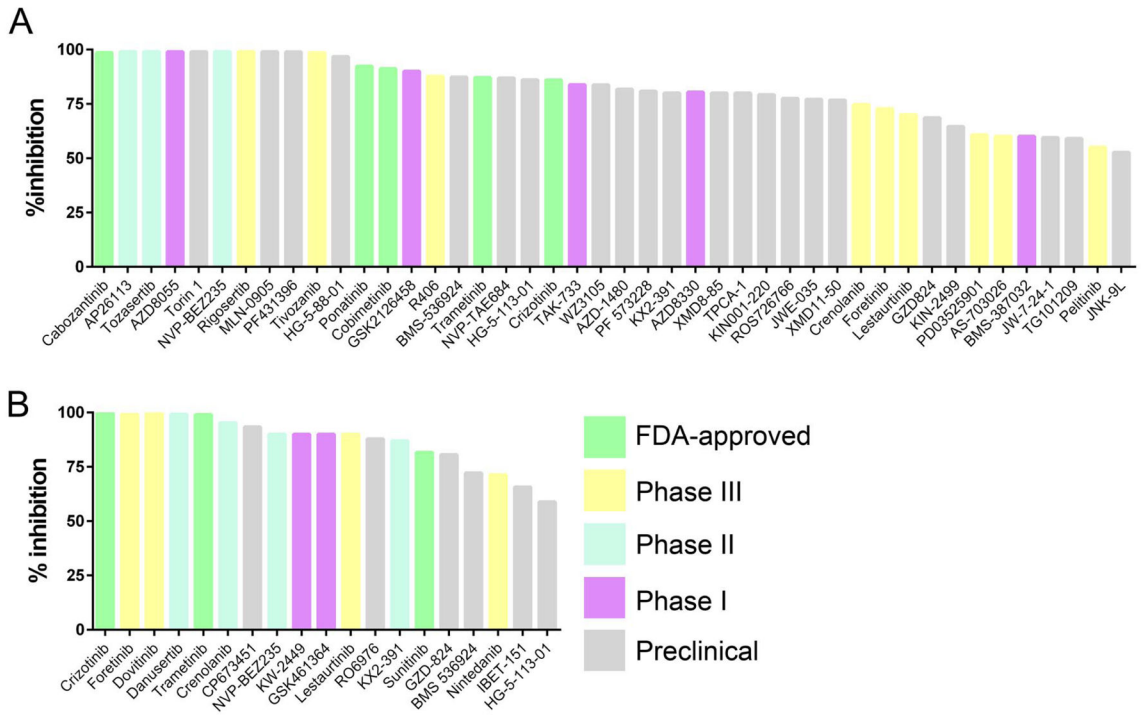

Figure 1.

A: Top inhibitors of Ba/F3 transformed with *CD74-ROS1*, color coded by clinical development status: FDA-approved (green), phase III (yellow), phase II (blue), phase I (purple), and preclinical (grey). **B:** Top inhibitors of Ba/F3 transformed with *CD74-NTRK1*, color coded by clinical development status: FDA-approved (green), phase III (yellow), phase II (blue), phase I (purple), and preclinical (grey).

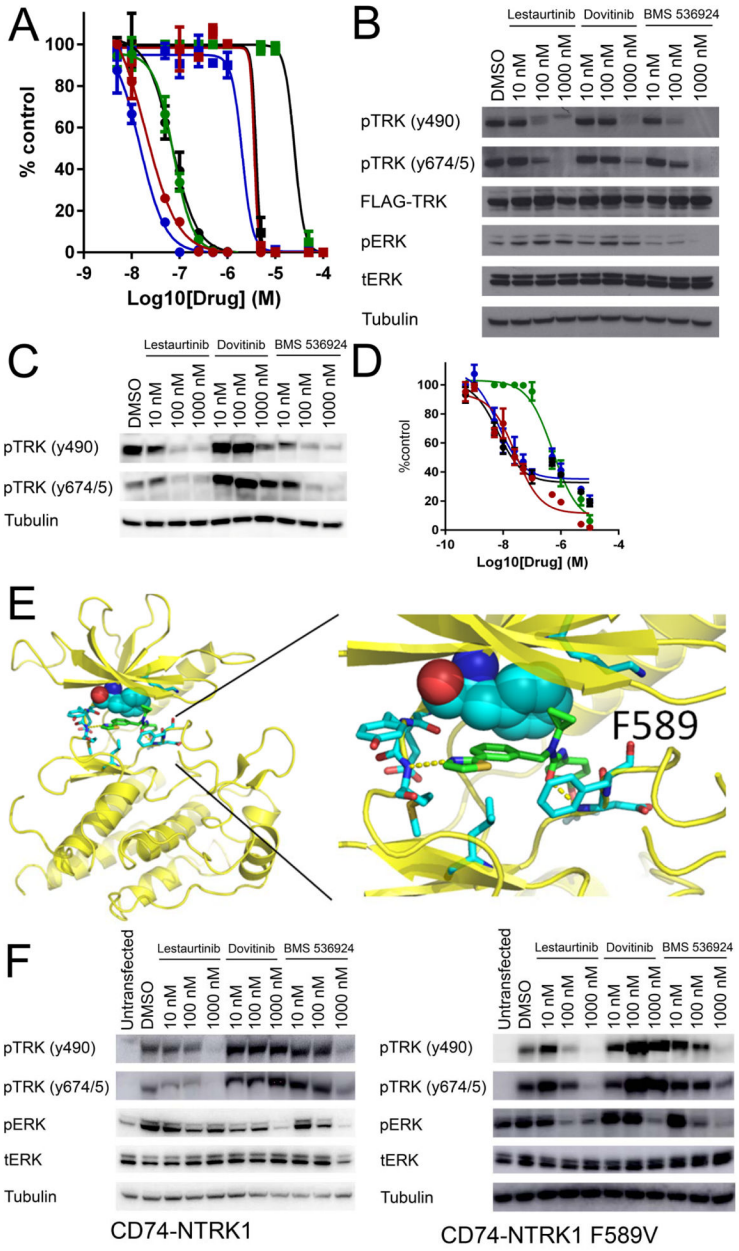

Figure 2.

A: Inhibition of Ba/F3 transformed with *CD74-NTRK1* proliferation by BMS-536924 (red, ●, IC_{50} = 28 nM), crizotinib (green, ●, IC_{50} = 75 nM), lestaurtinib (CEP-701, blue, ●, IC_{50} = 15 nM), and dovitinib (black, ●, IC_{50} = 69 nM) and of Ba/F3 parental cells by BMS-536924 (red, ■, IC_{50} = 2.75 μM), crizotinib (green, ■, IC_{50} = 15.4 μM), lestaurtinib (CEP-701, blue ■, IC_{50} = 3.4 μM), and dovitinib (■, IC_{50} = 4.2 μM). **B:** Inhibition of NTRK1 autophosphorylation and downstream signaling in *CD74-NTRK1*-transformed NIH-3T3 cells. **C:** Inhibition of NTRK1 autophosphorylation in CUTO-3 tumor cells derived from a patient harboring an *MPRIP-NTRK1* rearrangement. **D:** Inhibition of CUTO-3 cells by crizotinib (green, ●, IC_{50} = 462 nM), lestaurtinib (CEP-701, blue, ●, IC_{50}

= 3.5 nM), BMS-536924 (red, •, IC_{50} = 34 nM), dovitinib (black, ●, IC_{50} = 170 nM). **E:** Phe589 is postulated to be the "gatekeeper" residue in the NTRK1 kinase active site, and is modeled using space filling representation. **F:** Mutation of the putative "gatekeeper" residue Phe589 to Val does not abrogate inhibition of TRK autophosphorylation at residues 490 and 674/675 for lestaurtinib or BMS-536924.

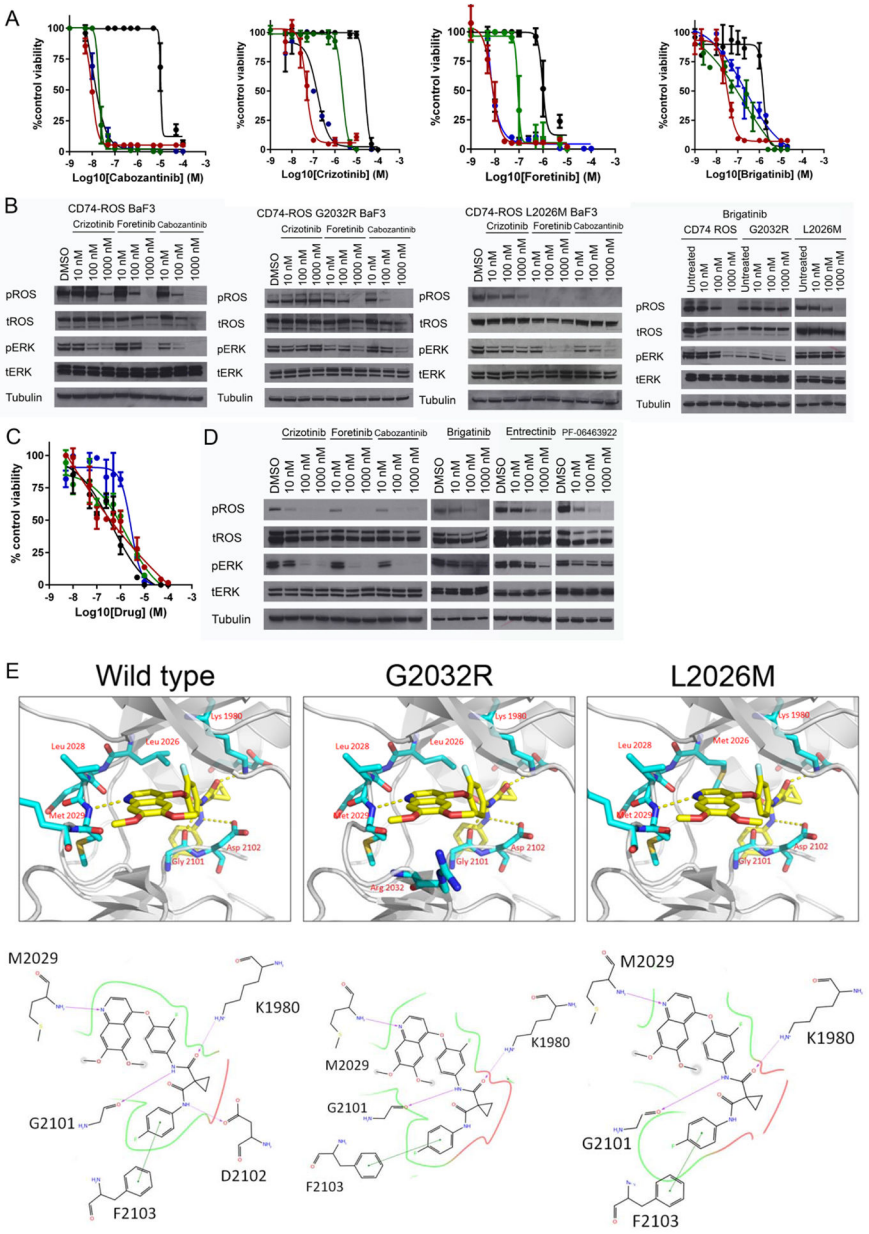

Figure 3.

A: Inhibition of Ba/F3 transformed with *CD74-ROS1* wildtype (red, ●), G2032R (green, ●), L2026M (blue, ●), and Ba/F3 parental cells (black, ●). **B:** Effect of drugs on ROS1 autophosphorylation (pY2274) and downstream activation of ERK signaling. **C:** Inhibition of the HCC78 NSCLC cell line by brigatinib (blue, ●, IC_{50} = 2.2 μM), cabozantinib (red, ●, IC_{50} = 1.36 μM) crizotinib (green, ●, IC_{50} = 1.6 μM), and foretinib (black, ●, IC_{50} = 0.46 μM); data for alectinib (IC_{50} = 0.75 μM), brigatinib (IC_{50} = 2.2 μM), ceritinib (IC_{50} = 0.53 μM), entrectinib (IC_{50} = 0.45 μM), and PF-06463922 (IC_{50} = > 10 μM) not shown. **D:** Inhibition of ROS signaling in HCC78 cells. **E:** Molecular modeling of cabozantinib into the active site of ROS1 kinase domain, with dashed lines indicating hydrogen bonds.

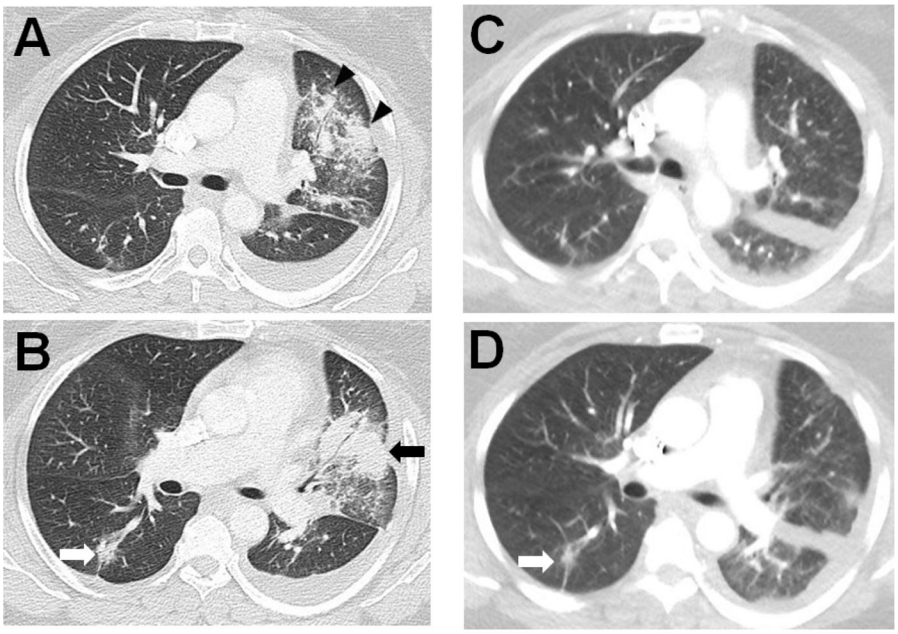

Figure 4.

A and B Computed tomography (CT) of the chest prior to cabozantinib therapy demonstrated a dominant mass in the left upper lobe (B, black arrow), measuring 4.3 cm in the longest diameter with patchy opacities (A, arrowheads) and a 1.7 cm discrete nodule in the right lower lobe (B, white arrow). Note bilateral small pleural effusions. **C and D:** On a chest CT scan performed due to dyspnea 4 weeks after the initiation of cabozantinib therapy, the the dominant lesion and surrounding tumor burden in the left upper lobe has mostly resolved with minimal residual opacities (C), indicating marked response to therapy. The right lower lobe lesion has also decreased, measuring 1.4 cm (arrow, D). Bilateral segmental pulmonary emboli are also noted (not shown), accounting for the clinical symptoms.

Table 1

Inhibition of Ba/F3 cells transformed with *CD74-ROS1* kinase

IC_{50} (μM)	Wild-type ROS	G2032R	L2026M	Parental Ba/F3	[Plasma] (μM)
Alectinib	> 10	> 10	4.2	> 10	1.4 (600 mg)
Brigatinib	0.03	0.17	0.2	1.54	N/A (Phase I/II)
Cabozantinib	0.009	0.026	0.011	> 10	1.08
Ceritinib	0.23	2.2	0.09	> 10	1.4
Crizotinib	0.044	2.7	0.127	> 10	0.61
Entrectinib	0.006	2.2	3.5	> 10	N/A
Foretinib	0.008	0.09	0.008	2.1	0.34–0.9
PF-06463922	0.001	0.27	0.002	> 10	N/A (Phase I)